SC 1004-A (2-54)

[redacted]

UNCLASSIFIED

Technical Memorandum

[redacted]

SANDIA SYSTEMATIC DECLASSIFICATION REVIEW
WITH LADING OR DECLASSIFICATION STAMP

CLASSIFICATION CHANGED TO: U	AUTHORITY: W. H. Lawrence
Emilda Selph 1-12-98	RECORD ID: 98SN0564
CHANGING MARKING & DATE: William Lorpe 1-12-98	DATED: 11-12-97
PERSON VERIFYING MARKING & DATE	

SC-TM-191-55-51

SOUND PULSE APPROXIMATIONS TO BLAST LOADING (WITH COMMENTS ON TRANSIENT DRAG)

C. C. HUDSON, 5112

SANDIA SYSTEMATIC

1st Review Date 11-06-97	Classification U
Authority ☐ ADD ☒ ADD W Lorpe	Comments
2nd Review Date 11/12/97	Comments
Authority ADD Name W.H. LAWRENCE	Comments O.K. for OPEN-NET

ABSTRACT

The equations of sound-pulse theory are used to calculate the overpressure pulses on the fronts of targets with the major assumptions of (1) a plane, ideal, shock wave; (2) diffracted waves from only nearest edges; and (3) no signal from rear of target. Both point overpressure pulses and average overpressure pulses are found. Corresponding experiments from both Coyote Canyon and Operation GREENHOUSE show good to excellent agreement with theory. The significance to transient drag of the overpressure on the front of the target is noted.

[redacted]

Case No. 408.01

UNCLASSIFIED

August 3, 1955

[redacted]

[redacted]

UNCLASSIFIED

DISTRIBUTION:
W. A. MacNair, 5000
S. C. Hight, 5100
E. F. Cox, 5110
R. W. Shephard, 5120
G. E. Hansche, 5140
M. L. Merritt, 5111
J. D. Shreve, 5112
W. D. Wood, 5122
S. H. Dike, 5123
W. Bleakney, Princeton University
C. W. Lampson, BRL
G. K. Hartmann, NOL
R. J. Hansen, MIT
N. M. Newmark, U. of Illinois
J. S. McNown, U. of Michigan
R. L. Corsbie, USAEC/DBM (3)
Lt. Col. E. E. Pickering, AFSWP, Washington, D.C. (2)
Commander, FC/AFSWP, Sandia Base (2)
Attn: Lt. W. J. Francy, Dev. Div.
Commander, FC/AFSWP, Sandia Base (3)
Attn: Adjutant General
For transmittal to:
Office of Naval Research
Department of the Navy
Washington 25, D.C.
Attn: Joseph Keller

Chief, Bureau of Yards and Docks
Department of the Navy
Washington 25, D.C.
Attn: Cmdr. Arthur B. Chellton, Jr.

U. S. Naval Civil Eng. Research and Evaluation Laboratory
U. S. Naval Construction Battalion Center
Port Hueneme, California
Attn: Cmdr. Victor G. Stevens, OIC

Martin D. Kirkpatrick, OCE
F. Genevese, AFOIN-ATD
E. H. Wang, WADC, WPAFB, Attn: WCRRN
S. J. Fraenkel, ARF
Max Linn, 1923 (6)
R and D Files, 1922-2

UNCLASSIFIED

[redacted]

TABLE OF CONTENTS

	Page
CHAPTER 1 - INTRODUCTION	4
Background	4
Setting up the Problem	4
CHAPTER 2 - THEORETICAL DEVELOPMENT	6
Determination of the Wave Length	6
Calculation of Point Overpressures	8
Comparison with Experiment: Point Overpressures	10
The Space-Time Diagram	12
CHAPTER 3 - NUMERICAL CALCULATIONS	15
Sound-Pulse Synthesis	15
Average from the Space-Time Diagram	16
Comparison with Experiment: Average Overpressures	18
Full-Scale Test	18
CHAPTER 4 - THE TRANSIENT DRAG QUESTION	20
Sound-Pulse Calculation of Drag: Asymptotic Value	20
Drag for a Decaying Wave	24
Numerical Calculations	27
CHAPTER 5 - CONCLUSIONS	27

LIST OF ILLUSTRATIONS

Fig. 1 -- Equivalent target for diffraction	5
Fig. 2 -- Contours of $p(\sigma, \eta)/p_m$ from acoustic theory	31
Fig. 3 -- Pressure pulses from Coyote Canyon experiments	11
Fig. 4 -- An experimental space-time diagram	13
Fig. 5 -- A sound-pulse space-time diagram	14
Fig. 6 -- Pressure pulses for the sound-pulse interaction	17
Fig. 7 -- Average pressure pulses for Coyote Canyon experiments	19
Fig. 8 -- Average pressure pulse for GREENHOUSE	21
Fig. 9 -- Point pressure pulses for GREENHOUSE	22
Fig. 10 -- Elastic part of drag coefficient	28

CHAPTER 1 -- INTRODUCTION

Background

There are some problems involving the interaction of blast or shock waves with obstacles which are sufficiently similar to the corresponding acoustic problem that, to learn pressure distributions, one need not begin with differential equations, but may instead proceed by similarity directly from acoustic or semi-acoustic solutions. The present problem, that of the diffraction of a blast wave by a rectangular target, is, in certain respects, of this type. We shall be talking about waves in which the increase in pressure is less than one atmosphere, known as "weak" waves, but with no limit on duration.

The basic principles of the sound-pulse approximation to shock diffraction were set down in the first End Effects report[1]. We shall now put these principles to use in computing the overpressures that result when a plane shock wave having the pulse shape

$$\Lambda(\sigma) = \frac{\overset{*}{p}(\sigma)}{\overset{*}{p}_m} = (1 - \sigma) \exp(-C\sigma) \tag{1}$$

impinges normally upon the front wall of a rectangular target. In Eq 1, $\overset{*}{p}_m$ is the peak overpressure of the incident wave, σ is a variable Vt/λ[†], and C is a decay constant. The asterisk is used to signify "incident wave".

Setting Up the Problem

We assume that the ground the target rests upon is a perfectly reflecting plane. Then, since incidence of the blast is taken as normal to the front face, the interaction may be simulated by allowing the wave to impinge upon a free block in space, as shown by Fig. 1. The dimensions of the block length a, height 2b, and breadth c. The overpressure at any point on the front surface is given approximately by[1]

$$\frac{p(t)}{\overset{*}{p}_m} = f(\sigma, \eta) = 2 + \frac{6\,\overset{*}{p}_m\,\Lambda(\sigma)}{\overset{*}{p}_m\,\Lambda(\sigma) + 7P_o}\,\Lambda(\sigma) - \sum_i f(\sigma, \eta_i) \tag{2}$$

where effects of fluid flow at the edges of the target are being ignored.

The symbol $f(\sigma, \eta_i)$ means a function corresponding to $\Lambda(\sigma)$ which represents the shape of the diffracted pulse. Again $\sigma = Vt/\lambda$ and $\eta = X/\lambda$ where λ is the "wave length" of the incident pulse. We will calculate its magnitude in the next chapter. The wave length is obtained for the incident pulse only and is used throughout to give a common length scale to the whole

† At this point we take time arbitrarily zero at the pulse front. Time for the interaction will be discussed in more detail later.

[redacted]

UNCLASSIFIED

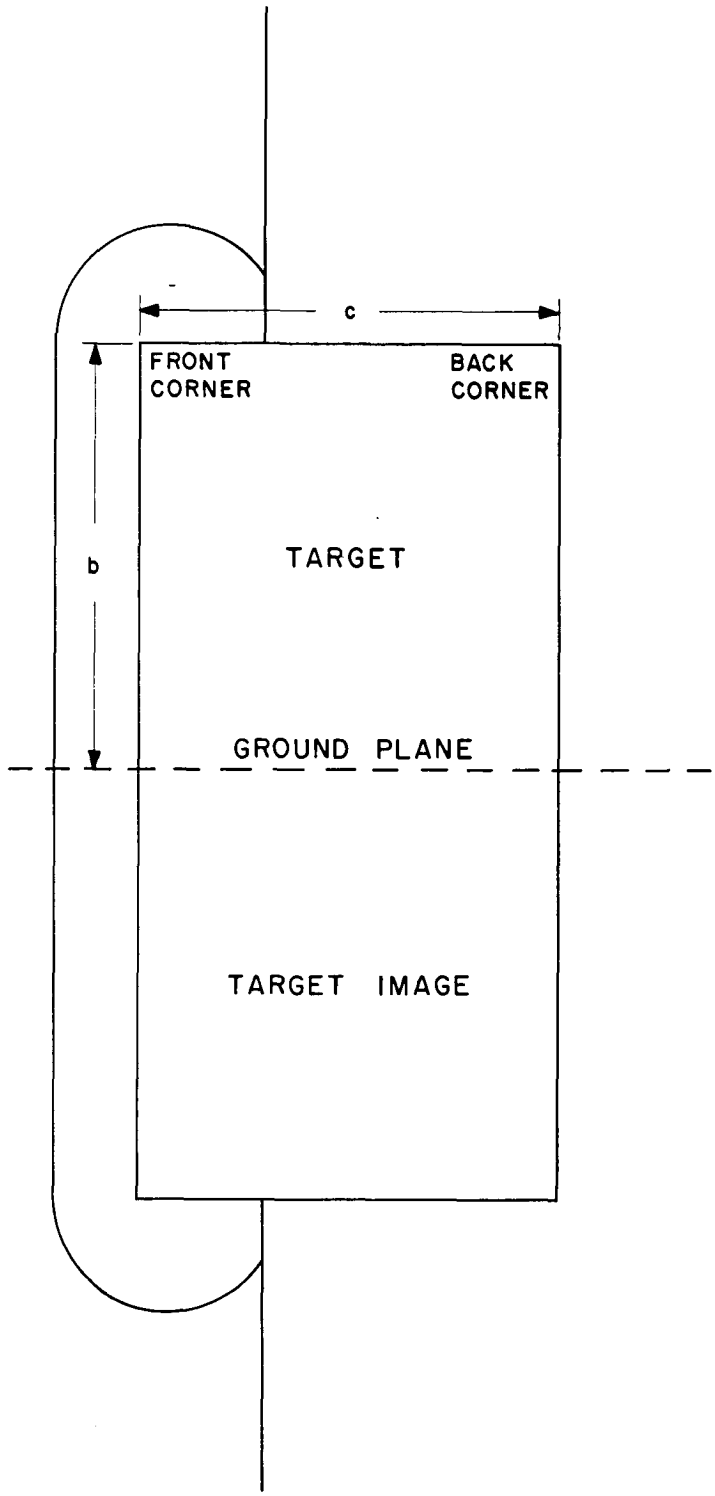

UNCLASSIFIED

Fig. 1 -- Equivalent target for diffraction

[redacted]

problem; it does not indicate the length of the diffracted waves. The dimensionless function $f_i(\sigma, \eta)$ gives the shape of the diffracted pulse (that is, the profile of the diffracted wave) as it moves along a radius from the source. Here we think of η as a parameter and σ as the independent variable so that $f(\sigma, \eta_i)$ is the σ profile of the wave at η_i.

The quantities V, t, and X are propagation velocity, time after the incident wave strikes the diffracting edge, and distance along the radius, respectively. In general V = V(t) but σ is invariant; that is, in different interactions the normalized pressure in the wave is the same for constant σ. We choose the radius to lay along the face of the target so that X_i actually denotes the position of a point on the target relative to a certain diffracting edge.

The position of the field point on the front surface is given by (X, Y) where X is the distance from the left edge and Y is the distance from the top edge. There are diffracted waves arriving at the point (X, Y) from all four edges of the front. The relative distances are given by

$$\eta_1 = X/\lambda$$
$$\eta_2 = Y/\lambda$$
$$\eta_3 = (a - X)/\lambda$$
$$\eta_4 = (2b - Y)/\lambda$$

where λ is the wavelength of the pulse. These numbers, $\eta_1 \ldots \eta_4$, will tell us how the shapes of the diffracted waves have changed in moving from their origin to the point in question. We introduce the Sommerfeld-DeWitt acoustic function for $f(\sigma, \eta)$[1, App C] which has been calculated and is presented in comprehensive form in Fig. 2. This figure, along with Eqs 1 and 2 will constitute our working tools for this problem.

CHAPTER 2 -- THEORETICAL DEVELOPMENT

Determination of the Wavelength

We shall define the characteristic length of the wave motion as the length of the positive phase of the incident wave when measured in the ground system as if the target were not there. This length becomes the measuring unit for the interaction; it will presently be shown that this is a sliding scale, variable in time.

Imagine that we are moving with such speed that the shock front is always at rest in our system. From this vantage point, we can look back and see the tail of the wave (i.e., the place where the pressure first falls to ambient). This tail slowly recedes with time because the head

and tail of the wave move with speeds U and a_o, respectively, with respect to the ground, a_o being ambient sound speed.

Now consider a marker fixed in the ground system (for instance, the target). The times at which the head and tail of the wave coincide with it are, respectively, t_1 and t_2. The distance measured will be exactly

$$\lambda(t_2) = \int_{t_1}^{t_2} U(t)\, dt, \tag{3}$$

and the λ at any time will be given closely* by

$$\lambda(t) - \lambda(t_1) = [U(t_2) - a_o](t - t_1). \tag{4}$$

In particular, at $t = t_2$

$$\lambda(t_1) = \lambda(t_2) - [U(t_2) - a_o]\,(t_2 - t_1) \tag{5}$$

so that

$$\lambda(t) = Q(t_2)\left[\frac{Q(t)}{Q(t_2)} + \frac{\int_{t_1}^{t_2} U(t)\, dt}{Q(t_2)} - 1\right] \tag{6}$$

where $Q(t) = [U(t) - a_o](t - t_1)$. If U(t) does not vary much between t_1 and t_2, we note that

$$\lambda(t) \approx U(t - t_1) + a_o\,(t_2 - t), \tag{7}$$

which is Ut_+ at t_2 or $a_o\, t_+$ at t_1, where $t_+ = t_2 - t_1$. For stronger waves, the characteristic length λ must be evaluated more accurately.

Sound-pulse theory specifies that a disturbance in a changing wave propagates with speed V such that

$$\vec{V} = \vec{a} \pm \vec{u}, \tag{8}$$

depending upon the sign of the gradient, a being the local sound speed and u the local fluid speed. It also chooses a characteristic length λ relative to which the distance moved by the disturbance may be noted. The variable is, therefore, $\sigma = Vt/\lambda$. The speed of any gradient within the incident shock wave lies between U and a_o. Thus

$$\begin{aligned} a_o < V < U \qquad & t_1 < t < t_2 \\ a_o\, t_+ < \lambda < Ut_+ \qquad & t_1 < t < t_2 \end{aligned} \tag{9}$$

but if the variation of V and λ is not marked (and for weak waves it is not), we may neglect it and for the incident wave write

$$\sigma = t/t_+.$$

---

* The tail of the overpressure pulse does not move exactly at ambient sound speed but the discrepancy here is not significant for our purpose.

It is now necessary to reduce σ for the diffracted waves also to a form involving explicitly the ratio t/t_+. Our justification for this seemingly arbitrary phrasing is to exploit the fact that here the pulse nature of the interaction is more important than minor changes in propagation speed. This is to say that the error $\Delta\sigma/\sigma$ due to changes in V is small:

$$\text{max error} = \frac{U - a_o}{U} << 1.$$

Under such conditions the diffracted pulses do not suffer significant nonlinear changes in shape while propagating, and $\frac{V}{U} \longrightarrow 1$ closely.

Calculation of the Point Overpressure

Let us now obtain for two experimental examples[1, 2] the overpressure measured as a function of time at a point on the front face.

The η, as mentioned before, determines the shape of the diffracted pulse; looking back at Fig. 2, one sees that when η is very small the diffracted pulse has essentially the same shape as the incident pulse and as increases the shape of the diffracted pulse becomes more round, weaker, and longer. Early in the interval $(t_2 - t_1)$ the diffracted pulse has about the same length as the incident.

According to Eq 2, the overpressure at a point is equal to the sum of the overpressures associated with the incident and reflected waves

$$2 + \left(\frac{6\overset{*}{p}_m}{\overset{*}{p}_m + 7P_o}\right)$$

and those associated with the diffracted waves $f_i\ (\sigma, \eta)$ in their proper phase relationships.

These phase relationships are rather complex, but within certain limits they can be simplified. In terms of σ, there is no problem; it is a variable incorporating changes in both propagation velocity and characteristic length in ratio so that differences between various partial waves are self-compensating. However, to relate sound-pulse theory to experiment, a single time scale must be arrived at which is easy to use. The interval $(t_2 - t_1)$ marks out the part of the interaction with which we are interested. Early in this interval (one might say "at the head of the incident wave") the diffracted waves move into an area of stagnation. Their fronts (where they do not interact) travel exactly with local sound velocity. In the region behind a reflected shock, this speed is

$$\left(\frac{a}{a_o}\right)^2 = y_r\left(\frac{y_r + 6}{1 + 6y_r}\right) \approx \frac{4/3\ y^2 + 7}{7} \tag{10}$$

which, it turns out, is nearly identical to the incident shock speed

$$\left(\frac{U}{a_o}\right)^2 = \frac{1 + 6y}{7} \tag{11}$$

for y greater than 1 but less than about 3. The approximation is the result of neglecting 7 relative to $48\,y^2$.

The distance traveled by the diffracted wave front during the interval t_1 to t_X is

$$X = \int_{t_1}^{t_X} a(t)\,dt \tag{12}$$

where the shock hits the front at time t_1. Since a(t) is almost constant during the early part of the interval, $X = a(t_X - t_1)$, and using the equivalence of a and U, the η_X denoting the arrival of the wave is

$$\eta_x = \frac{X}{\lambda} \approx \frac{U(t_X - t_1)}{\lambda}. \tag{13}$$

In the same part of the interval, σ, the time variable for the diffracted wave is

$$\sigma = \frac{Vt}{\lambda} \approx \frac{at}{\lambda} \approx \frac{Ut}{\lambda} \qquad t_X < t < t_2$$

where we have neglected the motion of the fluid caused by the diffracted (rarefaction) wave itself.

As previously noted, λ at the head of the wave (time t_1) is about $a_o\,t_+$ so

$$\begin{aligned} \eta_x &= \left(\frac{U}{a_o}\right)\frac{(t_X - t_1)}{t_+}, \\ \sigma &= \left(\frac{U}{a_o}\right)\frac{t}{t_+} \qquad t_X < t < t_2. \end{aligned} \tag{14}$$

The basic unit of time measure that we would like to use is t/t_+, which would be the same as the unit for the incident wave. Here it is multiplied by a quantity (U/a_o) which has a magnitude $\left(\frac{1 + 6y}{7}\right)^{1/2}$.

Note in the interval (at the tail of the incident wave), the propagation speed for the diffracted waves is more like a_o, ambient sound speed, so since $\lambda = Ut_+$,

$$\sigma = \frac{a_o}{U} \cdot \frac{t}{t_+} \tag{15}$$

the reciprocal of the other value. Somewhere in the middle of the interval, $\sigma = t/t_+$. If we take this value for simplicity, we will be making an error toward too long times at the head of the interval and too short times at the tail. But for weak waves, the error is small and not worth correcting.

We have now reduced our problem to a true sound-pulse representation in terms of p/p^*_m and t/t_+ with propagation speed U. From this point on, we may take $t_1 = 0$ to simplify the description.

Comparison with Experiment: Point Overpressures

Let us now use Fig. 2 to make up pulses equivalent to those measured in some actual tests. The target was 6 feet square and 36 feet long[1, 2], and the X_i's are given in the order

X_1 = distance from leading edge
X_2 = distance from image of leading edge
X_3 = distance from nearer end
X_4 = distance from farther end.

This notation is more functional and is not intended to follow that of Chapter 1. Table I gives the pertinent data.

TABLE I

Shot No.	Gauge No.	C	p_m^* (psi)	t_+ (msec)	X_1 (ft)	X_2 (ft)	X_3 (ft)	X_4 (ft)	η_1	η_2	η_3	η_4
M-11	4	1.15	7.5	47	4	8	17-1/4	18-3/4	0.06	0.12	0.261	0.284
M-11	8	1.15	7.5	47	1	11	17-1/4	18-3/4	0.015	0.067	0.261	0.284
H-2	9	1.2	8.5	58	2	10	1	35	0.024	0.122	0.012	0.427

The incident and reflected overpressures are given by the first term of Eq 2 using Eq 1 to give $\Lambda(\sigma)$. The functions so computed are plotted in Fig. 3. Then from Fig. 2 the normalized diffracted overpressures are read off at constant η as a function of σ. These overpressure pulses are subtracted from the curve just plotted. They are put in the correct phase by commencing at $\eta_i t_+$ after the front of the pulse; the η_i are given in Table I. The complete pulses are shown in Fig. 3. The heavy line gives the effective overpressure at the point. This compares rather well with the experimental curve (the dotted line) during the first part of the pulse.

The two curves, theoretical and experimental, for M-11 diverge at about $t/t_+ = 0.26$, or 12 msec, which is too soon to expect positive pulses returning from the rear of the target. Therefore we must conclude that the rarefaction waves arriving from the ends of the target have been greatly weakened compared with values predicted by a two-dimensional diffraction theory; this is due simply to divergence (lack of confinement) at the upper edge of the wave.

As an approximation, we may write from our experience that the pulse associated with a wave having traveled more than the length of the originating edge is negligible. Thus, for M-11, the measured overpressure is given essentially by Eq 2 using just the first two diffracted waves, while in H-2 where pressure stations were closer to the end, three diffracted waves must be used. Our rule of thumb must be taken for the moment as empirical. It gives a simple means of deciding which waves to use.

[redacted]

UNCLASSIFIED

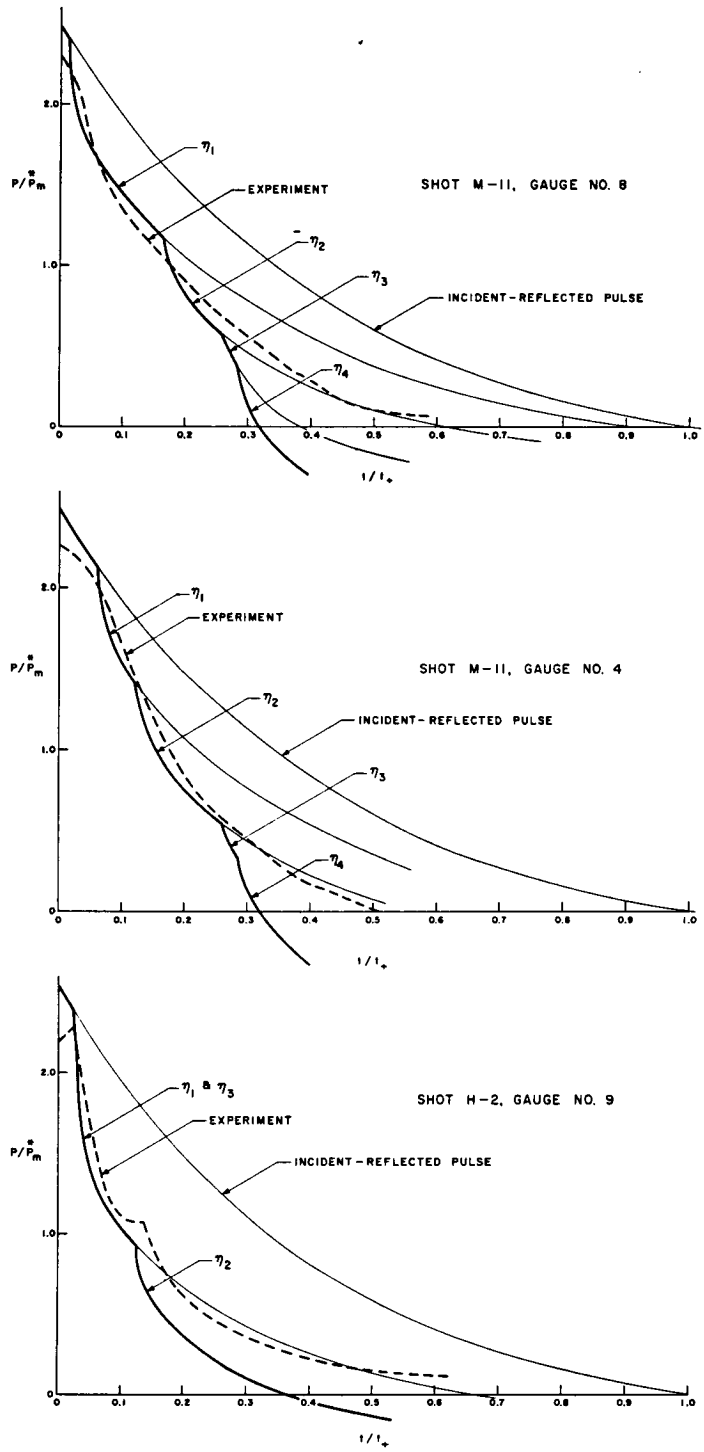

UNCLASSIFIED

Fig. 3 -- Pressure pulses from Coyote Canyon experiments

[redacted]

It is important to comment on an assumption in our synthesis, an assumption that becomes very significant when long shock waves hit small targets. We have assumed that the target is so deep in the direction of motion of the wave that no signals from the rear of the target reach the front during the positive-phase duration such as was the case at Coyote Canyon[1,2]; but for most nuclear explosions this is not a realistic attitude. Chapter 4 in this report gives a brief examination of the question.

The Space-Time Diagram

The complete picture of the overpressures developed on the front of the target is given by the space-time diagram of this area. The diagram is discussed in detail in the End Effects reports[2,3] and briefly amounts to plotting overpressure contours (or some other physically significant variable) so that they describe the events in one direction across a surface of the target as a function of time. The experimental overpressures (corrected for gauge aberrations) were plotted directly in terms of distance (feet) and time (msecs) in these reports. Figure 4 (M-11) is a typical example. Here we shall synthesize the diagram from a knowledge of the target geometry, the incident wave, and the sound-pulse theory. In fact, Fig. 2 is a space (η) -time (σ) diagram of the propagation of a single diffracted (rarefaction) wave.

As an example, let us choose an idealized situation where the dimension b of the (two-dimensional) target is $\eta_o = b/\lambda = 0.10$;* this will compare closely with the M-11 example where $\eta_o = 0.09$. The diagram (Fig. 5) is made with axes η and σ, where η is essentially X, the distance from the leading edge, and σ is essentially t, time after the shock hits the front surface. Due to the condition that the plane incident wave strikes the plane target surface normally, the instantaneous peak overpressure at any η due to the incident and reflected waves above is given by the first term of Eq 2.

We have also calculated the σ - η diagram for the back of this target (Fig. 5). The errors involved in this process are in general greater than those for the front because waves on the back (a) change their shape during propagation and (b) are not as strong, relatively speaking, as the waves on the front. Nonetheless, there are occasions when such calculations are appropriate, as will be shown in Chapter 4.

On the front, a rarefaction wave from the leading edge passes diagonally through the field, intercepting the line $\eta = 0.10$ at $\sigma = 0.10$ (Fig. 5). The image wave, having started in an imaginary space, now enters the diagram as the reflected wave and passes through the field

* η_o is used as a parameter characteristic of the interaction since it relates the size of the target to the size of the wave. Usually the chosen dimension of the target is the smaller of the two dimensions of the face most directly hit by the incident wave.

[redacted]

UNCLASSIFIED

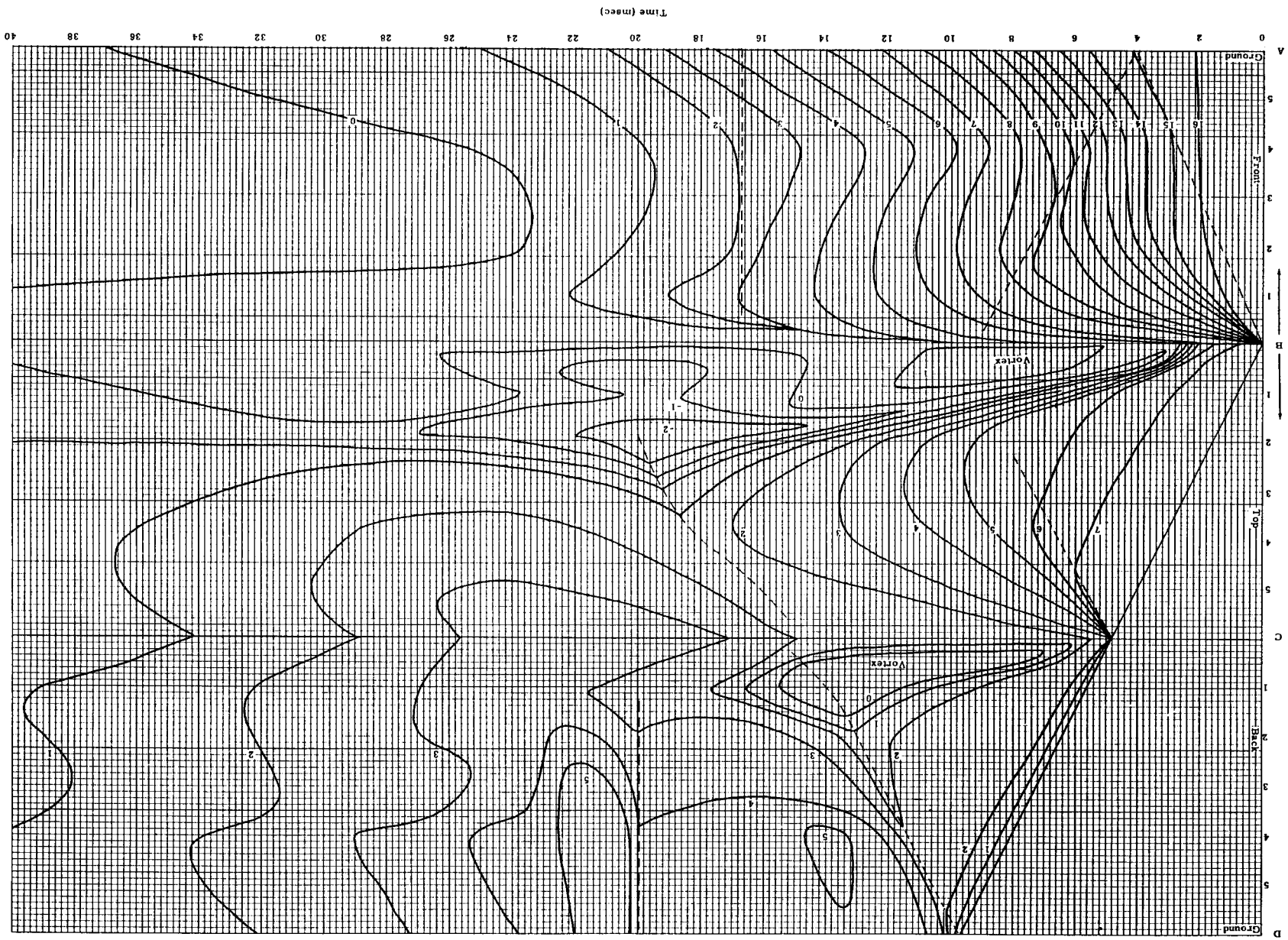

Fig. 4 -- An experimental space-time diagram

[redacted]

UNCLASSIFIED

[redacted]
UNCLASSIFIED

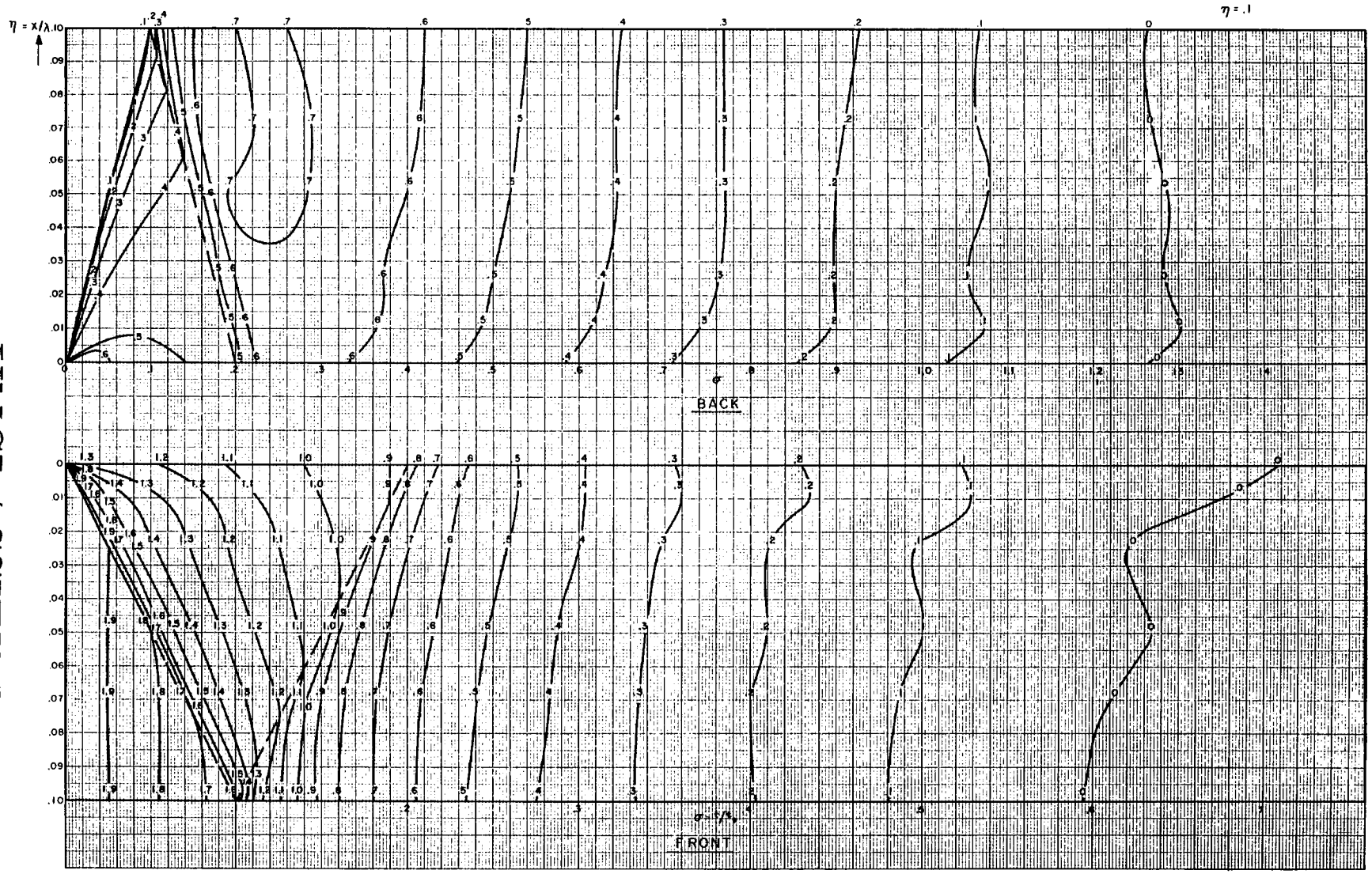

Fig. 5 -- A sound-pulse space-time diagram

[redacted]
UNCLASSIFIED

to $\sigma = 0.20$ at $\eta = 0$. These features are shown by the dotted lines in Fig. 5. We shall assume that no further signals are pertinent and proceed to compute the pressures behind the wave fronts.

CHAPTER 3 -- NUMERICAL CALCULATIONS

Sound-Pulse Synthesis

We shall now describe in detail how to construct such diagrams. On the assumption that we may synthesize directly from Eq 2 with constant propagation velocities, our working formula is given by

$$\Gamma(\sigma, \eta) = \frac{p(t/t_+)}{\overset{*}{p}_m} = \left[2 + \frac{6\overset{*}{p}_m(t/t_+)}{\overset{*}{p}_m(t/t_+) + 7P_o}\right]\Lambda(t/t_+) + f_1(t/t_+, \eta_1) + f_2(t/t_+, \eta_2) + f_3(t/t_+, \eta_3) + f_4(t/t_+, \eta_4) \tag{16}$$

where $\Lambda(t/t_+)$ is given by Eq 1 and the $f_1(t/t_+, \eta_1)$ by Fig. 2. We may compute either at constant t/t_+ or at constant η. Calculating overpressures around the target at constant t/t_+ is analogous to photographing the density variations as is done in the shock tube whereas calculating at constant η is analogous to making a measurement of pressure as a function of time, such as is done by physically locating a pressure gauge on the target.

It is again pertinent to note that Fig. 2 was constructed for $C = 1.0$ (Eq 1) and therefore is not exact for interactions where the incident wave has other values of the decay constant. However, we have computed diffraction problems with different values of C (work not yet published) and the effect of variation in C for values near unity is very small, becoming noticeable only as $C \rightarrow 0$ or as C exceeds 5. We feel that the errors introduced by a variation $0.5 < C < 2.0$ are minor compared with errors brought in by other approximations.

We must now deal with the phase relationships involved in combining several diffracted waves with the pulse due to the incident and reflected waves. We will make use of the example just described. Suppose we wish to compute the resultant overpressure pulse at a given value of η in the space-time diagram, Fig. 5. The arrivals of the diffracted wave fronts relative to t_+ are given by $\eta_1 = X_1/\lambda$, $\eta_2 = X_2/\lambda$, etc, for as many diffracted pulses as are to be used. The overpressure (normalized by $\overset{*}{p}_m$) at any position behind a given diffracted wave front, i.e., at $\delta_i = \sigma - \eta_i$, is obtainable from Fig. 2. The diffracted waves begin at $t = 0$, coincident with the hitting of the face of the target by the shock front. In other words, σ is our basic, independent variable; we choose σ's at intervals of, say, 0.1, and for each value add up the

components of the incident-reflected pulse and the (negative) diffracted pulses. When no $\sigma - \eta_i$ has a value greater than zero, no diffracted wave can have arrived at that station. If $\sigma - \eta_i > 0$, then the ith wave has arrived and contributes to the resultant overpressure.

Figure 6 shows the pressure-σ curves at various values of η for the $\sigma - \eta$ diagram of Fig. 5. These were obtained with the use of the curves of Fig. 2. To form the $\sigma - \eta$ diagram, equal pressures were read from these drawings and plotted in Fig. 5. Notice that this front space-time diagram is very similar to that of Fig. 4, dealing with a (measured) shock interaction, except that in the latter the contours at $\eta = 0$ all turn back toward earlier σ. This turning is accountable to the finite flow of fluid around the corner which, by the Bernoulli effect, lowers the pressure in the stream. In other words, a given pressure near the edge is found earlier with finite flow than with no flow.

In remarking about this discrepancy, we would like to point out that the complete sound-pulse solution contains a velocity term which at the edge goes to $\rightarrow\infty$, in the classical tradition. We have omitted the term on the grounds that the actual flow is relatively small and the large negative values of classical theory are not justified. *

Average from the Space-Time Diagram

When the space-time diagram for a line on the front surface has already been drawn or when, as for experimental work, it must be drawn, a numerical method for obtaining the average pressure is already available.[4] For sound-pulse work, however, it is not necessary to complete the diagram if all that is desired is the average pressure. For example, let us consider how to obtain the average pressure along a line on the front face parallel to the end of the target, a situation often actually encountered. At any σ, the pressure-distance relationship along this line is found from Eq 2 by the use of the diffracted wave data of Fig. 2. Taking η's at equal intervals across the face $\eta_m = b/\lambda$, where b is the height of the face, we have by the trapezoidal rule,

$$\left(\frac{\bar{p}}{p^*_m}\right)_{\sigma\ \mathrm{const}} = \frac{\Delta\eta}{\eta_m}\left[1/2\ \Gamma 0 + \Gamma 1 + \Gamma 2 \ldots \Gamma_{n-1} + i/2\ \Gamma_n\right] \tag{17}$$

where the terms Γ_i are the values of the sound-pulse function at the various intervals. Each of these terms is an individual application of Eq 2 and Fig. 2, uniquely given by

$$\Gamma_i = \Gamma(\sigma, \eta_i).$$

* A vortex forms at the edge which forces air flow to go around a new blunt contour; actual air speeds are not very high at the edge.

UNCLASSIFIED

[redacted]

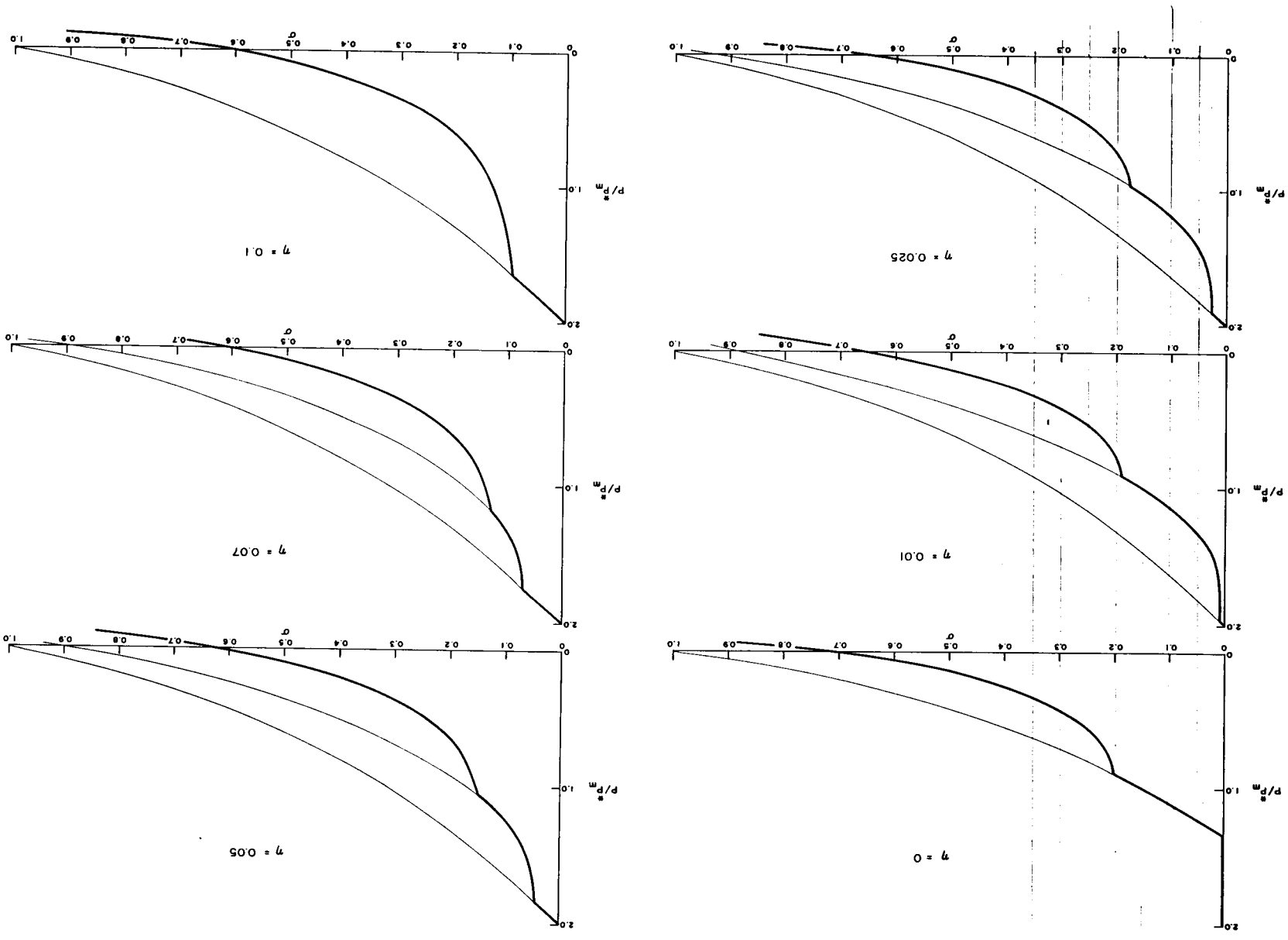

Fig. 6 -- Pressure pulses for the sound pulse interaction

[redacted]

UNCLASSIFIED

Repeating this computation for enough σ's defines the average pressure-time curve for the line. Choosing enough lines appropriately would permit obtaining the average pressure-time function over any desired area of the target face.

Comparison with Experiment: Average Overpressure

Figure 7 shows the sound-pulse average pressure functions for shots M-11[1] and H-2[2] along with the actual average overpressure functions obtained from these experiments. The M-11 curve includes the effects of 2 diffracted waves, and that of H-2 includes also the effect of the third diffracted wave from the target end only 5 feet away. The shaded area represents the usual $\pm$ 5 per cent error of the field measurements; but the sound-pulse curves, on this same scale, are essentially without error. A small discrepancy almost always exists in the establishment of the maximum overpressure.

Clearly the sound-pulse calculation is a satisfactory means of predicting the average overpressure-time function in the case of Coyote Canyon experiments at these pressure levels when the target is large enough to make the assumption of negligible fluid flow at corners tenable.

Full-Scale Tests

The chief purpose of both the sound-pulse theory and the Coyote Canyon experiments is to permit us to estimate with engineering accuracy the pressure pulses that are applied to real targets in full-scale explosions. We naturally expect such great explosions to present rather complex interplay of various physical effects.

There have been, however, only a few full-scale tests which could be used for evaluation purposes and of these only one had a ratio b/λ great enough to be of interest; that is, when the ratio b/λ is too small, the decaying nature of the pulse becomes unimportant. Structure 3.1.1 (36 x 52 x 194 feet) on Operation GREENHOUSE was hit almost normally on the front face by a shock wave having approximately the parameters $\overset{*}{p}_m$ = 12.5 psi, t_+ = 830 msec and C = 2/3. The radius of the shock was so great compared with the size of the target that the wave front could be considered plane.

The gauge records from this experiment were individually difficult to interpret for several reasons: (1) there was some evidence of electronic circuitry malfunction; (2) there was an indication that the front of the target was aflame when the shock arrived and how much effect this had on the propagation of aerodynamic disturbances is not known; (3) since the target was not a simple one, local disturbances undoubtedly played a part in modifying the overpressure pattern. However, even though no one gauge can be trusted, the whole set of gauges that measured the movement of the system of waves over the target does give a rather good picture of the interaction. Thus a space-time diagram was composed[3] and from it one is able

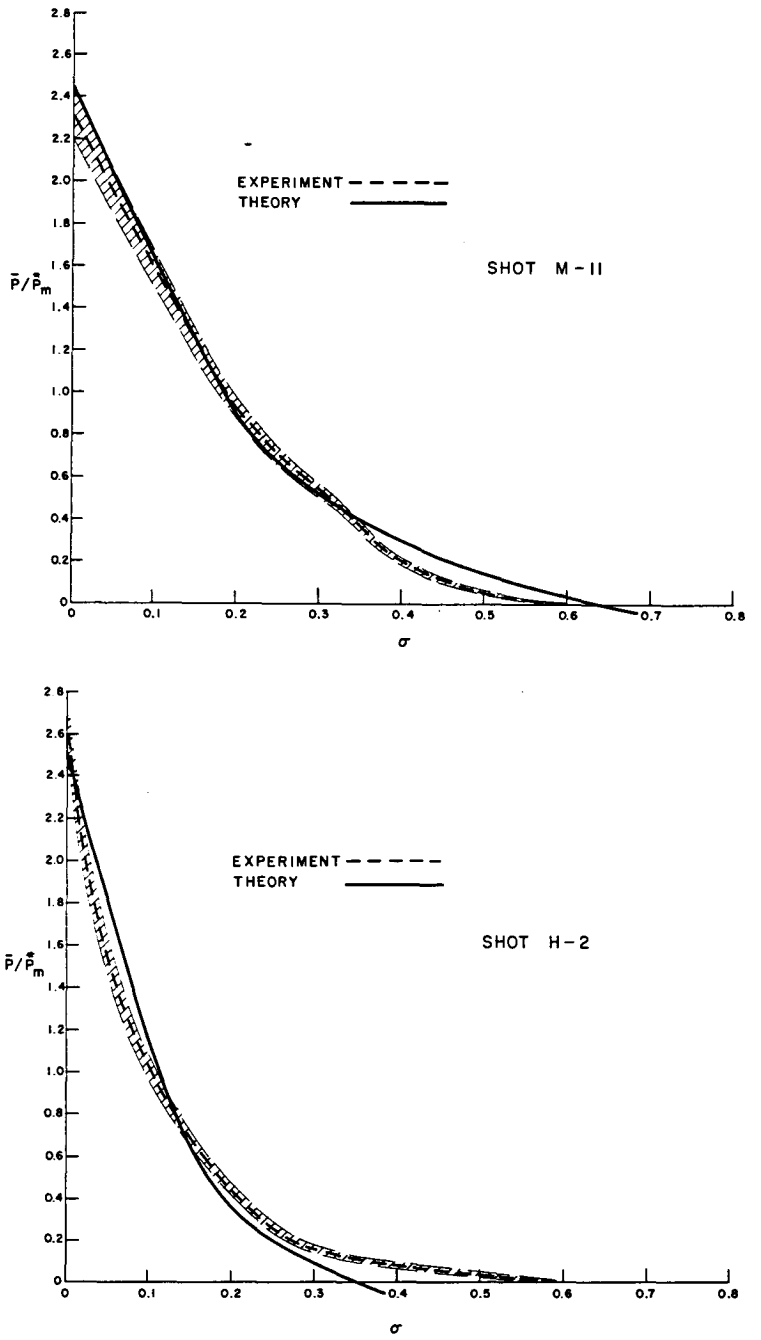

Fig. 7 -- Average pressure pulses for Coyote Canyon experiments

to obtain an idea of the pressure applied on a part of the target's surface at about 60 feet from one end. The average of the space-time diagram was taken surface by surface, and the average overpressure on the front of the target is shown in Fig. 8. On the same scale, we have presented two sound-pulse estimates, one including waves from the target ends and one not. Again the effect of the end waves is exaggerated. Notice that the reflected shock from the ground behind the target would have been felt at about $\sigma = 0.25$ (arrow in drawing). Before this time, only rarefaction waves are present; afterwards, the situation becomes more complex as waves pass back and forth. There is apparently some small contribution from the end waves to the real pressure; our rule of thumb would neglect them altogether.

We have computed the point overpressure on the front for two actual gauge positions. Figure 9a shows a gauge near one end where three diffraction waves were important. Agreement in magnitude is not good although timing appears to be satisfactory. Here again we are uncertain both as to the gauge reading and to the necessary end corrections. Figure 9b shows the best (front) gauge in the set that contributed the space-time diagram. We have (by rule of thumb) ignored the end waves. Agreement is satisfactory.

CHAPTER 4 -- THE DRAG QUESTION

Sound-Pulse Calculation of Drag: Asymptotic Value

Let us assume that the principal contributions to drag are the average front and back overpressures, then we have

$$\text{Drag} = \left(\bar{p}_f(t) - \bar{p}_b(t)\right). \tag{18}$$

We further make the assumption that

$$\text{Drag} = C_D \overset{*}{q} = C'_D \overset{*}{p} \tag{19}$$

where $\overset{*}{q}$ and $\overset{*}{p}$ are the dynamic pressure and static overpressure, respectively. Then

$$C'_D = (\bar{p}_f - \bar{p}_b)/\overset{*}{p} \tag{20}$$

which we shall now calculate from sound-pulse theory for a flat-topped wave.

It has previously been pointed out that in a real situation, the diffracted wave upon encountering an edge is diffracted around it but a negligible signal is sent back. We take this always to be true. Thus if the strength of the diffracted wave is z, its diffracted counterpart

UNCLASSIFIED

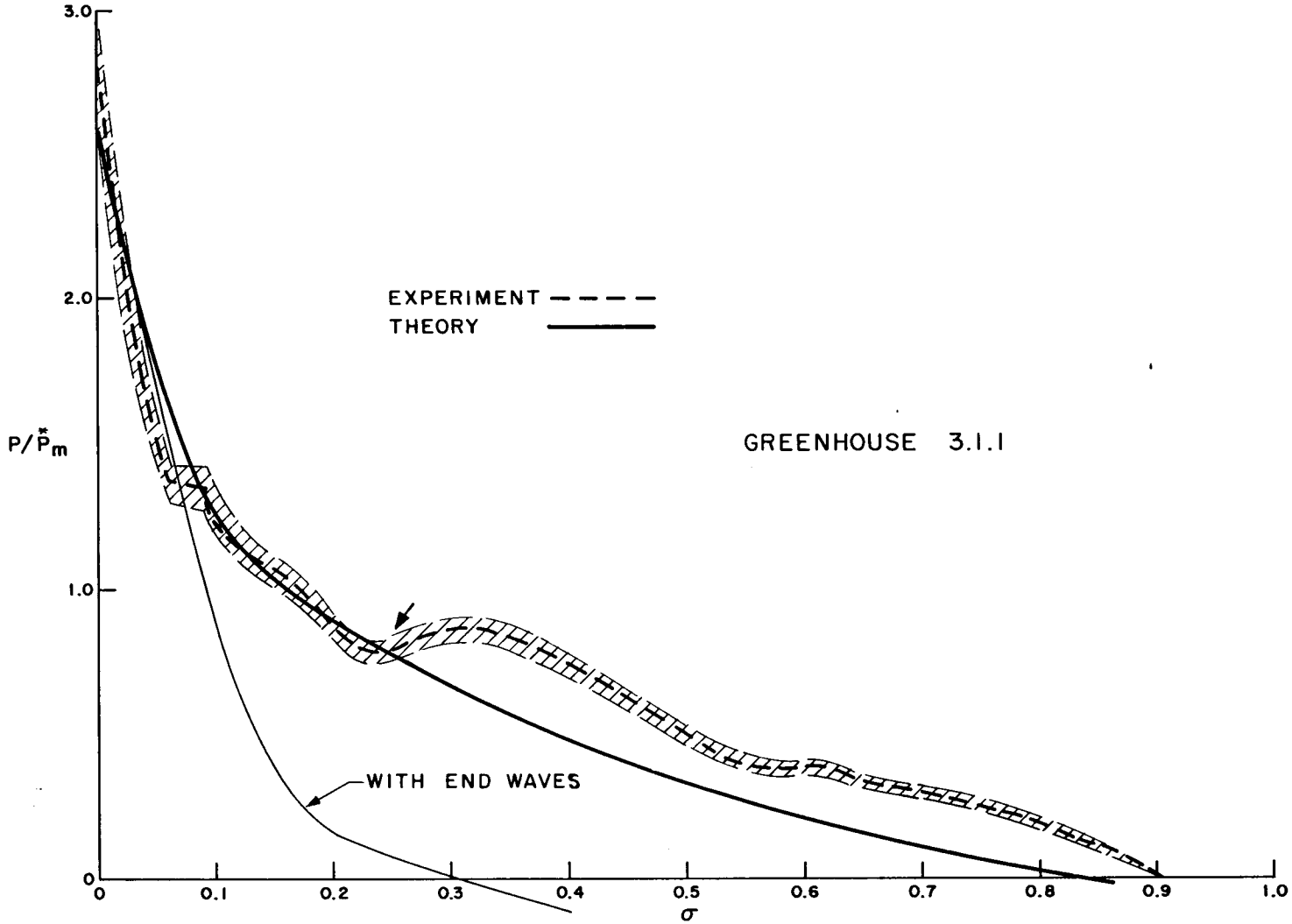

Fig. 8 -- Average pressure pulse for GREENHOUSE

UNCLASSIFIED

[redacted]

UNCLASSIFIED

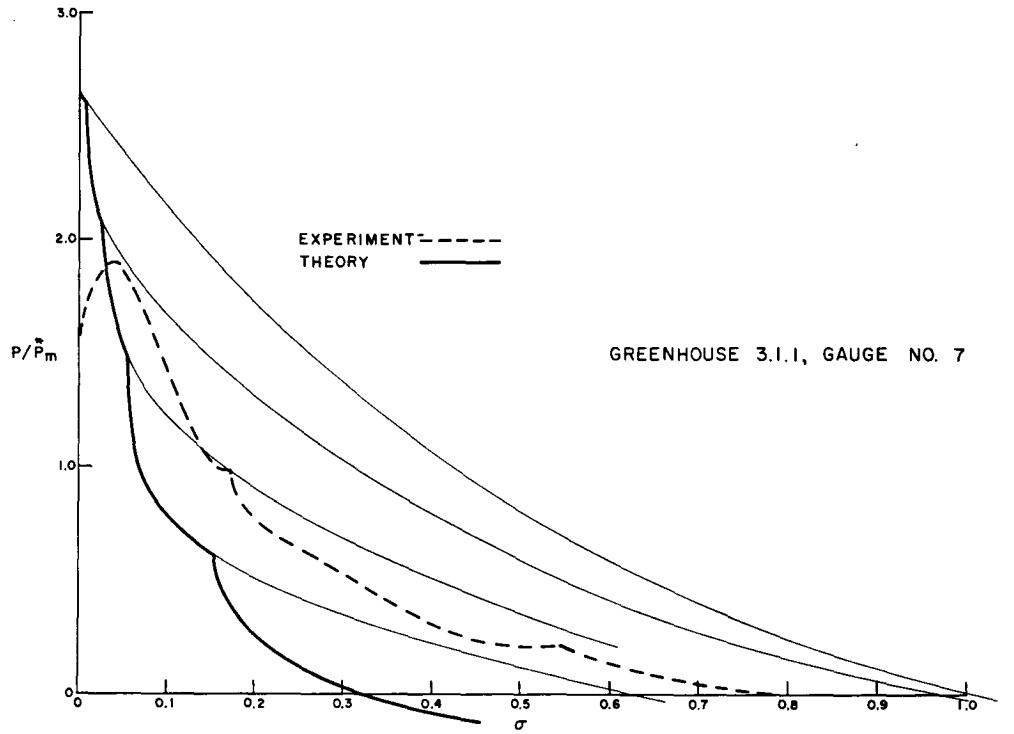

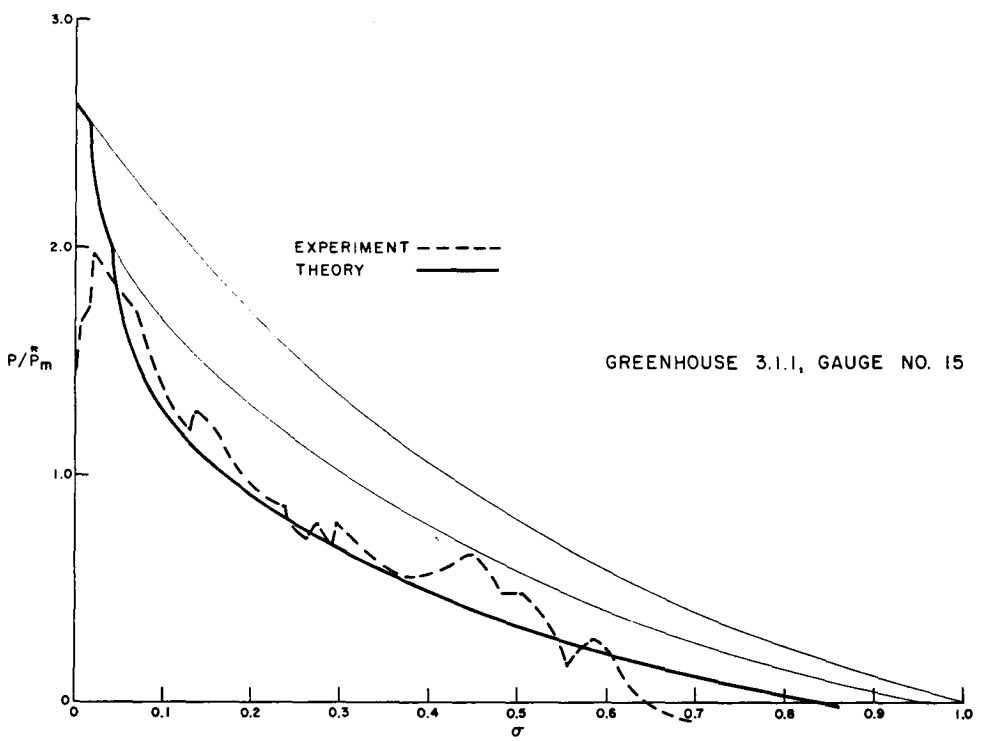

Fig. 9 -- Point pressure pulses for GREENHOUSE

UNCLASSIFIED

[redacted]

is $2/3\ z^{\dagger}$, the second diffraction gives $2/3 \cdot 2/3\,z$, and so on. For a flat-topped wave in the limit of $\sigma \to \infty$, we find on the front face the approximation to the average overpressure

$$\bar{p}_f/\overset{*}{p}_m = \left[2 + \frac{6(y-1)}{6+y}\right] + 2\left[-2/3 + 2/3 \cdot 2/3 \cdot 2/3 - 2/3 \cdot 2/3 \cdot 2/3 \cdot 2/3 \cdot 2/3 + \ldots\right] \tag{21}$$

and on the back

$$\bar{p}_b/\overset{*}{p}_m = 2\left[2/3 - 2/3 \cdot 2/3 \cdot 2/3 + 2/3 \cdot 2/3 \cdot 2/3 \cdot 2/3 \cdot 2/3 - \ldots\right] \tag{22}$$

The difference is merely the first bracket. The drag coefficient is then

$$C_D = \left[2 + \frac{6(y-1)}{6+y}\right]/K \tag{23}$$

where K is the ratio of dynamic pressure to static overpressure in the incident wave. It was found that in the first End Effects report[1] that (for $\gamma = 1.4$)

$$K = 2.5\,\frac{y-1}{y+6}\,. \tag{24}$$

Thus

$$C_D = \left[2 + 6\,\frac{y-1}{6+y}\right]/2.5\left(\frac{y-1}{y+6}\right) \tag{25}$$

$$= \frac{2}{2.5}\left[1/\left(\frac{y-1}{y+6}\right) + 3\right].$$

The wave analysis thus gives in a first approximation a drag coefficient of ∞ for $y \to 1^{\ddagger}$ and in the limit, $y \to \infty$, it goes to 3.2. This equation gives much too high values. The difficulty can be traced to the $6\left(\frac{y-1}{6+y}\right)$ term, which says that the nonlinear increase in overpressure at the target front due to stopping the blast wave persists as $\sigma \to \infty$. Partially the discrepancy is also

---

† DeWitt[6] has shown that the velocity potential of the diffracted wave is

$$\Phi = \frac{1}{\pi}\tan^{-1}\frac{\sin\epsilon\pi\sinh\epsilon b}{\cos\epsilon(\phi - \phi') - \cos\epsilon\pi\cosh\epsilon b}$$

in the region $\pi + \phi' < \phi < \pi/\epsilon$ where ϕ is the angle at the field point, ϕ' is the angle of incidence, $\epsilon = m/n$ and $b = \cosh^{-1}(\sigma/\eta)$. If we let $\sigma \to \infty$, $b \to \infty$ but the limit of the argument remains finite and is $\tan\epsilon\pi$. In our case $m/n = 2/3$ because the exterior angle of the wedge is 270°. Thus $\Phi = 2/3$. It was shown in the first End Effects report[1] that $\Phi = p/\overset{*}{p}_m$ so that the peak overpressure in the limit of small η approaches $2/3\overset{*}{p}_m$ for one diffraction. We call $2/3\,\overset{*}{p}_m = z$ the strength of the diffracted wave.

‡ From both theory and experiment the infinite limit at $y \to 1$ appears to be proper.

due to the assumption of no interference between front and back faces. We know experimentally that the limit is, instead, the stagnation or total pressure. In our case it consists of the static pressure present in the wave and the dynamic pressure. Thus the overpressure on the front, including the effect of the diffracted waves, goes to $1 + 2.5\left(\frac{y-1}{y+6}\right)$. The difference between this and the wave formula must be due to terms arising from flow alone, i.e.

$$\left[2 + 6\,\frac{y-1}{y+6}\right] + 2\,[-2/3 + 2/3 \cdot 2/3 \cdot 2/3 - 2/3 \cdot 2/3 \cdot 2/3 \cdot 2/3 \cdot 2/3 + \ldots] + R_f(y)$$
$$= 1 + 2.5\left(\frac{y-1}{y+6}\right) \tag{26}$$

The first part of this equation may be called the <u>elastic</u>† terms and $R_f(y)$ the <u>inertial</u> part.

Similarly on the back we should find

The series is written $-4/3\,[(-1)^0 + (-1)(2/3)^2 + (-1)^2[(2/3)^2]^2 + \cdots (-1)^m[(2/3)^2]^m + \cdots]$

$$2\,[2/3 - 2/3 \cdot 2/3 \cdot 2/3 + 2/3 \cdot 2/3 \cdot 2/3 \cdot 2/3 \cdot 2/3 - \ldots] + R_b(y) = \text{base overpressure}, \tag{27}$$

which has the sum $-(4/3)/1+(2/3)^2 = -12/13$

but unfortunately we do not know what the base overpressure ought to be. Making the assumption that the base overpressure is given by the elastic terms the drag coefficient becomes

$$C_D = \left[1 + 2.5\left(\frac{y-1}{y+6}\right)\right]/K = 1 + \frac{y+6}{2.5\,(y-1)}\,. \tag{28}$$

Then this becomes $\{1/13 + 2.5\left(\frac{y-1}{y+6}\right)\}/K$

Again at y = 1 (the acoustic limit) the drag coefficient goes to ∞ but at $y \to \infty$, it now limits at 1.40, which is a more reasonable range. Table III gives some values computed from this formula for various y.

TABLE III

y	1	2	3	4	5	10
C_D	∞	~~4.20~~	~~2.80~~	~~2.33~~	~~2.10~~	~~1.71~~
	∞	1.216	1.138	1.103	1.085	1.051

Actually this calculation of the drag coefficient is valueless for any practical work. It merely shows that for the case of a flat-topped (step) pulse acting on a long square member, in the $\sigma \to \infty$ limit, our drag coefficient has a reasonable range of values. The front overpressure is the dominant contribution to the drag. Note the inconsistancy in using only the elastic terms on the back as $\sigma \to \infty$.

Drag for a Decaying Wave

If we do not take the limiting case $\sigma \to \infty$ and if we look again at decaying waves, the problem becomes rather more complex. Let us consider both the elastic and inertial parts.

† This notation is due to Dr. John S. McNown, University of Michigan, consultant to Sandia Corporation.

The drag is now defined as

$$\text{Drag} = C_D \overset{*}{q}(\sigma) \tag{29}$$

where $\overset{*}{q}(\sigma)$ is the dynamic pressure in the incident wave as a function of σ (time). The front average overpressure is given by

$$\frac{\bar{p}_f}{\overset{*}{p}_m} = \left\{ \left[2 + \frac{6\, p_m \Lambda(\sigma)}{\overset{*}{p}_m \Lambda(\sigma) + \eta P_o} \right] \Lambda(\sigma) + \sum_i f_i(\sigma, \eta) + R_f(\sigma, \eta, \overset{*}{p}_m) \right\}_{\text{Ave}} \tag{30}$$

where now the inertial part R_f must consist of two types of terms, the usual one in V^2 and a new one in dV/dt† to account for the fact that the wave is decaying. The diffracted waves of all kinds are included in the $\sum_i f_i$ term and the phase relationships here must be carefully considered. The back average overpressure is given less accurately by

$$\frac{\bar{p}_b}{\overset{*}{p}_m} \approx \left\{ \sum_i f_i(\sigma, \eta) + R_b(\sigma, \eta, \overset{*}{p}_m) \right\}_{\text{Ave}} \tag{31}$$

where $f_i(\sigma, \eta)$ is the back wedge counterpart to the front wedge function already used and where $R_b(\sigma, \eta, \overset{*}{p}_m)$ stems from the flow associated with these waves. Neither of these quantities can be expected to be exact but at least one can hope to be able to calculate them eventually.

Digressing a moment, and going back to the interval $(t_2 - t_1)$, which designates the time of interaction, it seems obvious that early in the interval (near t_1 or at the head of the wave), the elastic terms will always be predominant. Now it appears that a certain relative time might be needed to set up the inertial flow. So if the ratio $\eta_o = L/\lambda$ is large, where L is the characteristic dimension of the target, then perhaps throughout the interval the elastic terms will dominate. But certainly, as η_o becomes smaller, there will be a transition from elastic to inertial terms and if η_o is small enough, the inertial terms will dominate the interval. We might present in these words the usual drag relationships (Table IV).

TABLE IV

η_o large	η_o medium	η_o small
Elastic	Elastic-inertial	Inertial
Pure diffraction	Mixed	Pure drag

† From Dr. John S. McNown.

Our asymptotic approximation to drag might be said to be in the η_o small limit. The most difficult range in which to calculate, and the most important in actual target analysis, is the middle range of mixed interaction. The Coyote Canyon experiments fall in the pure diffraction range. Note that in each case there is some diffraction and some drag. Our ranges merely indicate which effect dominates the interaction interval $(t_2 - t_1)$.

Returning now to the drag coefficient, it is calculated by

$$C_D(\sigma) = \frac{\bar{p}_f(\sigma) - \bar{p}_m(\sigma)}{\overset{*}{q}_m(\sigma)} \tag{32}$$

These quantities cannot be readily obtained algebraically, but we can get $\bar{p}_f(\sigma)$ and $\bar{p}_b(\sigma)$ by semigraphical procedures using the space-time diagram. We can then describe in general terms what $C_D(\sigma)$ must look like.

The first phase will depend only on the diffraction or elastic terms. The curve $C_D(\sigma)$ must begin at

$$\left[2 + 6\left(\frac{y-1}{y+6}\right)\right]/2.5\left(\frac{y-1}{y+6}\right) = 0.80\left(\frac{y+6}{y-1}\right) + \overset{2.40}{\cancel{1.20}} \tag{33}$$

and decrease rapidly to a minimum. The minimum is caused by the reflection of the compression wave at the back and its arrival at the front. Whether or not this minimum is negative depends upon the target depth. If waves from the rear are delayed long enough, the full effect of the rarefaction waves will be felt and the overpressure will go negative. If waves from the rear arrive sooner, they will more or less neutralize the effect of the rarefaction waves and the drag minimum will be less negative or may even be positive.

Following this minimum we should expect oscillations of rather large amplitude which rapidly die out. These oscillations are caused by the movement of the rarefaction and compression waves around the target out of phase. The period should be approximately 2τ[†] from a consideration of the interplay of the diffracted waves.

The final phase of the drag interaction is the leveling off of $C_D(\sigma)$ to a more or less steady value. At some time the dv/dt term should play a prominent role but eventually this effect should die out leaving the time-independent steady-state drag coefficient.

All of these phases may or may not occur within the positive phase interval $(t_2 - t_1)$ of the interaction. We have demonstrated that the first phase (ahead of the first minimum) is principally elastic in nature by showing that the elastic terms suffice as a means of arriving

[†] The dimensionless time unit τ is defined as t/t_x where t_x is the time required by the wave front to travel the height of the target, h/U.

at experimental results. While the diffracted waves are encircling the target, inertial effects begin to be set up as the waves die out (second phase) and eventually (third phase) the interaction is almost entirely inertial. Small-scale experiments do not give us clear-cut drag data when the second and third phases occur in the negative phase of the incident wave (that is, for times greater than t_2). Thus we must go to the full-scale tests for experimentation.

Numerical Calculations

By the methods outlined in this report one can arrive at a sound pulse estimate of the actual drag force at any section of the target. The estimate is, of course, best for weak blast interactions, best for only the first part of the interaction, and best either close to the target end or far from it, so that the divergence of the end waves is not an uncertainty. We have determined the drag coefficient to its first minimum for M-11, H-2, and GREENHOUSE 3.1.1 by sound-pulse methods. The measured drag coefficients (from the second End Effects report)[3] are given in Fig. 10; the calculated values are indicated by dashed lines. One should remember that the sound pulse calculation assumes no interference between front and back, which is not true for GREENHOUSE 3.1.1.

A preliminary effort to obtain the dv/dt effect has been made by Prof. John S. McNown of the University of Michigan. His result has been communicated (privately) to the author in the case of GREENHOUSE 3.1.1. The horizontal line in Fig. 10 is his estimate of the drag, using his corrections. The range of its applicability is not well fixed.

CHAPTER 5 -- CONCLUSIONS

We have tried to present in a simple manner the accomplishments of a similarity theory of blast diffraction. Mostly the theory has been developed intuitively, and its physical backgrounds are not very firmly established. Within the range of its application, however, it can serve as an engineering procedure. The tedious numerical and graphical work that is necessary to get, for instance, an average pressure-time curve can be eliminated entirely by the use of a simple electronic computor. A prototype has already been tested and has proved entirely satisfactory. In principle we can expect to be able to calculate any of the quantities described in this report in a matter of seconds with a machine as simple as a slide rule.

Many of the difficulties associated with this study will be remembered by the reader. Among them are:

(a) Restriction to incidence in the plane of the target cross section

(b) Omission of fluid flow

(c) Noninteraction of diffracted waves

[redacted]

UNCLASSIFIED

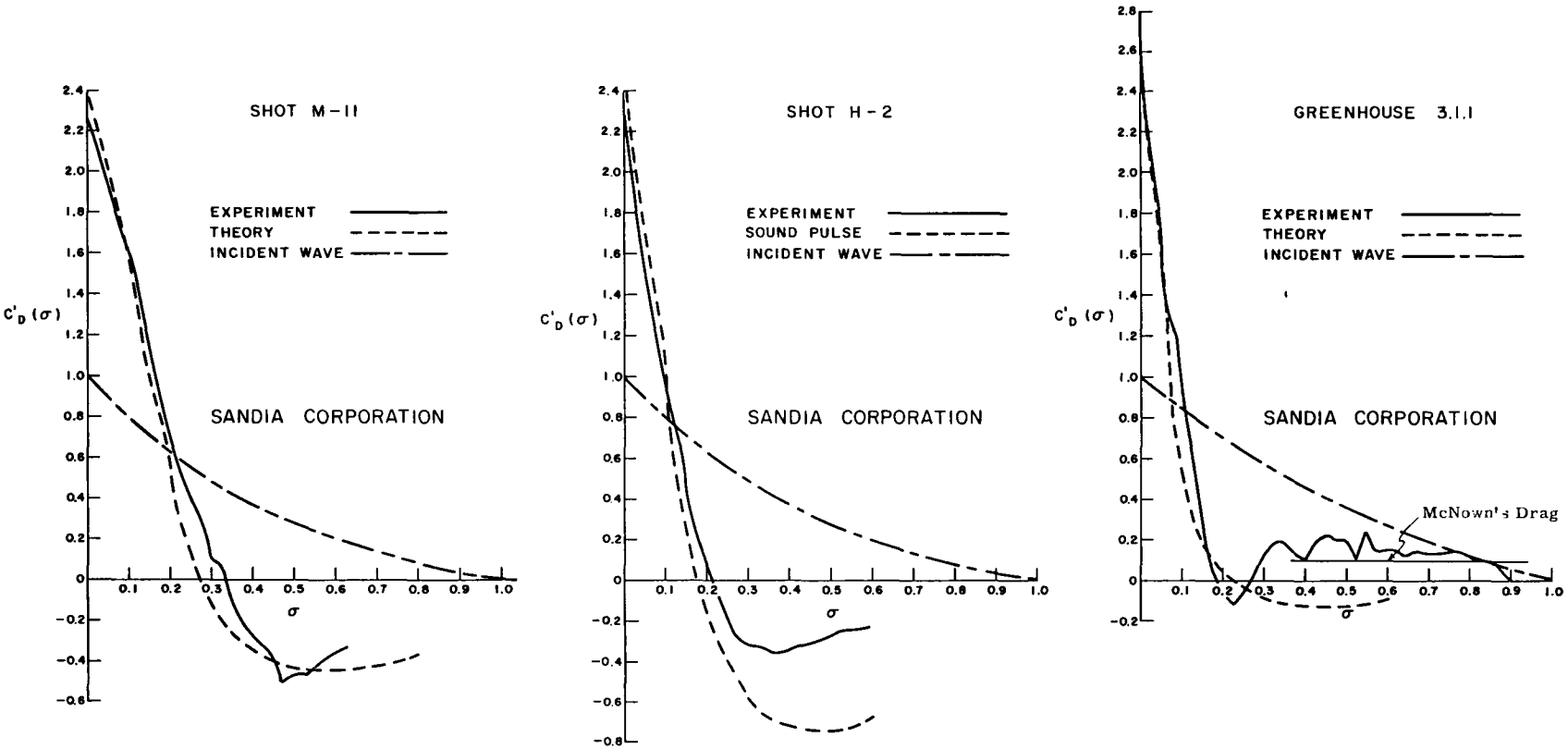

Fig. 10 -- Elastic part of drag coefficient

UNCLASSIFIED

[redacted]

[redacted]

UNCLASSIFIED

(d) Restrictions to weak waves

(e) No description of the transition from elastic to inertial states

(f) Divergence of end waves.

We are hoping to be able to set the theory on a more realistic physical foundation, at which time some of these difficulties will disappear.

C. C. HUDSON, 5112

Case No. 408.01
August 3, 1955

UNCLASSIFIED

[redacted]

[redacted]

UNCLASSIFIED

LIST OF REFERENCES

1. Hudson, C. C., Blast Loading End Effects I, AFSWP 461, August 24, 1954.

2. Merritt, M. L., Some Tests on the Diffraction of Blast Waves, Sandia Corporation Report SC-1803(TR), June 7, 1951.

3. Hudson, C. C., Blast Loading End Effects II, AFSWP 462, to be published.

4. Hudson, C. C., A Numerical Integration Scheme for Problems Involving Contour Representations, Sandia Corporation Technical Memorandum 138-55-51, July 6, 1955.

5. Merritt, M. L., Some Preliminary Results of a Study of Diffraction Around Structures at GREENHOUSE, Sandia Corporation memorandum Ref. Sym: 1112 (66), September 13, 1951.

6. DeWitt, H. E., Extension of the Sommerfeld Diffraction Theory to Wedge of Arbitrary Angle, Sandia Corporation Technical Memorandum 13-54-51, February 4, 1954.

UNCLASSIFIED

[redacted]

DECLASSIFIED

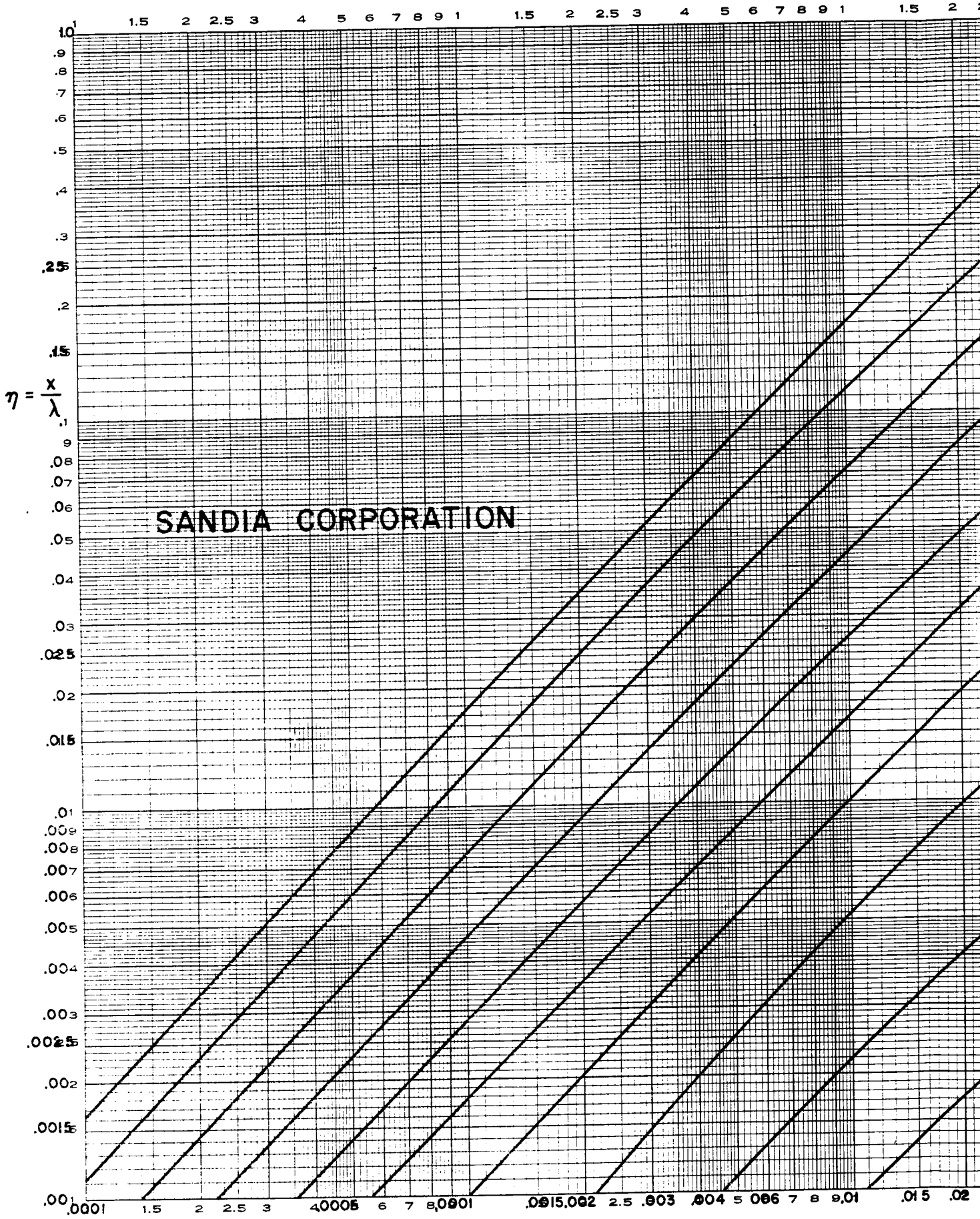

[redacted]

$\delta = \sigma$

Fig. 2 -- Contours of $P(\sigma$

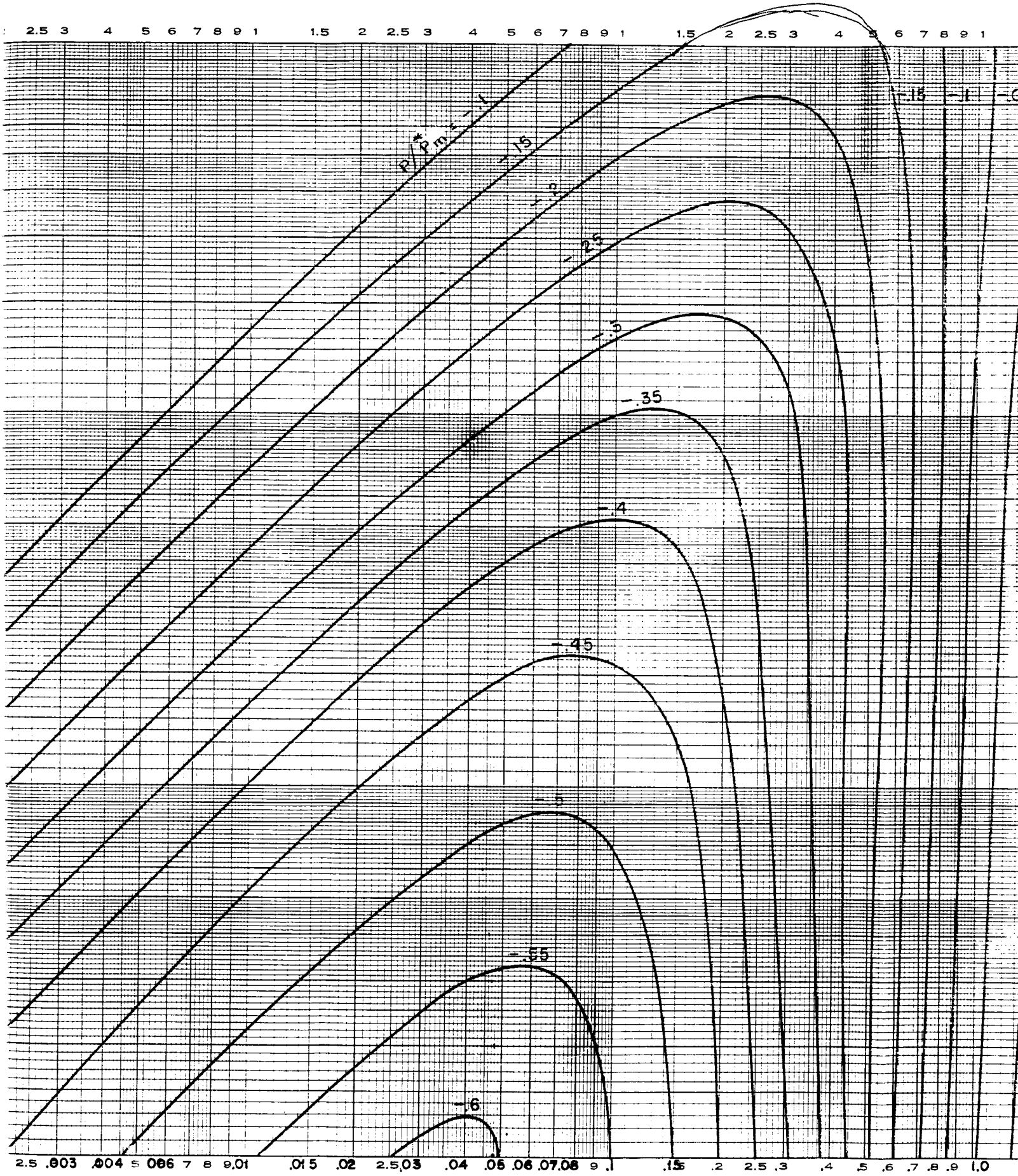

$$\delta = \sigma - \eta = \frac{Vt - x}{\lambda}$$

Fig. [illegible] Contours of [illegible]

[redacted]

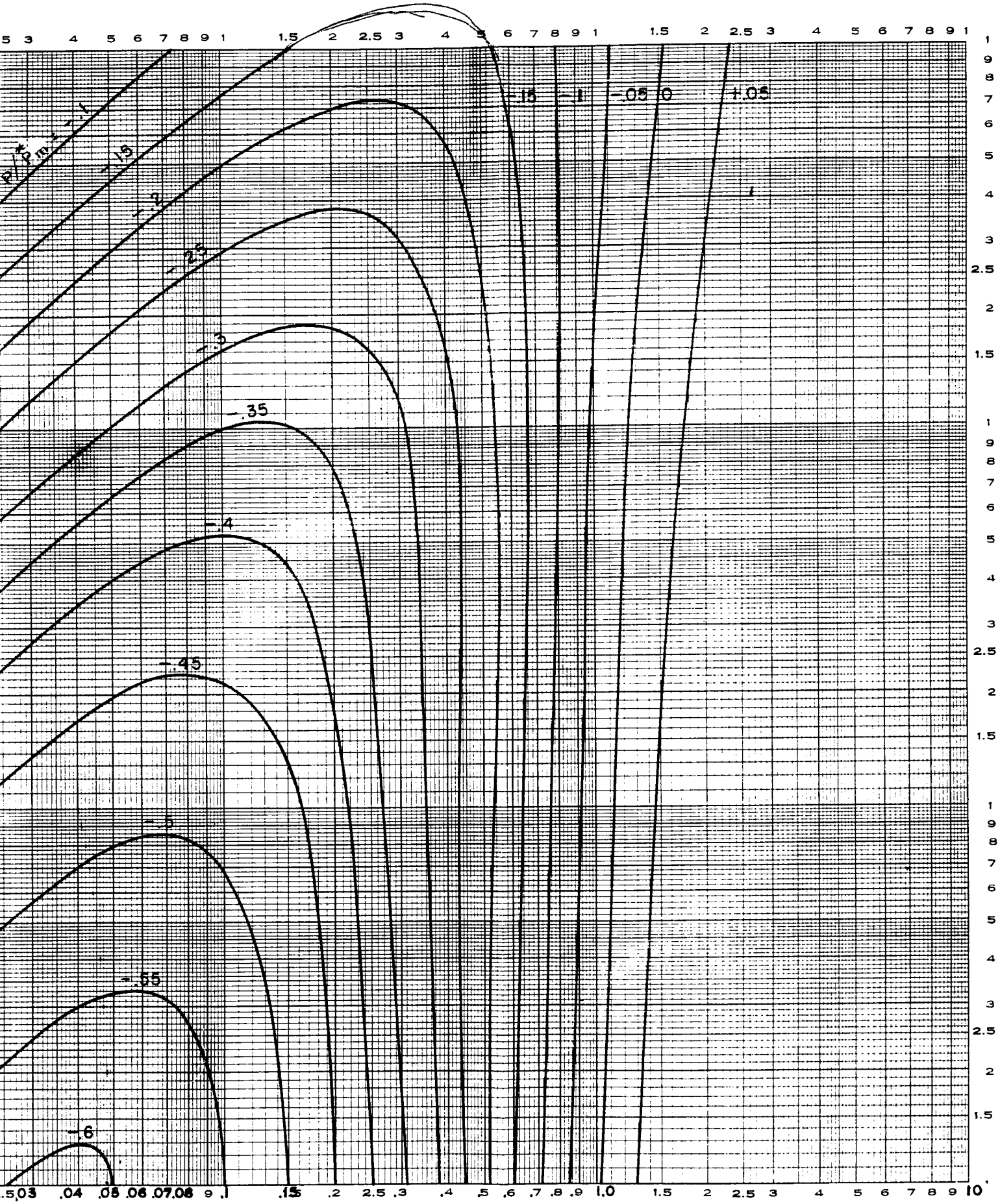

$$\eta = \frac{Vt - x}{\lambda}$$

$)/\overset{*}{p}_m$ from acoustic theory

FRONT FRONT

$\phi = 0°$, $\phi' = 90°$

UNCLASSIFIED